ARTICLE
PUBLISHED ONLINE: 12 SEPTEMBER 2016 | DOI: 10.1038/NCHEMBIO.2179

# A chemical-inducible CRISPR–Cas9 system for rapid control of genome editing

Kaiwen Ivy Liu[1], Muhammad Nadzim Bin Ramli[1], Cheok Wei Ariel Woo[1], Yuanming Wang[1,2], Tianyun Zhao[1], Xiujun Zhang[1,2], Guo Rong Daniel Yim[1], Bao Yi Chong[1,3], Ali Gowher[1], Mervyn Zi Hao Chua[1,4], Jonathan Jung[1], Jia Hui Jane Lee[1] & Meng How Tan[1,2]*

**CRISPR–Cas9 has emerged as a powerful technology that enables ready modification of the mammalian genome. The ability to modulate Cas9 activity can reduce off-target cleavage and facilitate precise genome engineering. Here we report the development of a Cas9 variant whose activity can be switched on and off in human cells with 4-hydroxytamoxifen (4-HT) by fusing the Cas9 enzyme with the hormone-binding domain of the estrogen receptor (ERT2). The final optimized variant, termed iCas, showed low endonuclease activity without 4-HT but high editing efficiency at multiple loci with the chemical. We also tuned the duration and concentration of 4-HT treatment to reduce off-target genome modification. Additionally, we benchmarked iCas against other chemical-inducible methods and found that it had the fastest on rate and that its activity could be toggled on and off repeatedly. Collectively, these results highlight the utility of iCas for rapid and reversible control of genome-editing function.**

© 2016 Nature America, Inc. All rights reserved.

New genome-editing technologies hold the promise to accelerate knowledge discovery and drug development. The CRISPR–Cas9 system, co-opted from bacteria, is particularly attractive because the elements that recognize the target genomic loci are single guide RNA (sgRNA) molecules, which are straightforward to design and synthesize[1–3]. The sgRNA recruits the Cas9 nuclease to the DNA to create a double-stranded break. Much effort has been devoted to improving the specificity of the Cas9 enzyme[4–16].

There are many applications in which it is imperative that the activity of Cas9 can be switched on and off as desired. For example, the ability to perturb regulatory networks in a particular tissue or at a specific time point is essential for understanding mammalian development. In cell signaling pathways, precise timing is also of paramount importance. One possible approach to create a conditional genome-editing system is to express Cas9 under an inducible promoter or a promoter that is active only in particular biological contexts[17–20]. However, such an approach has several disadvantages. First, the response time is typically slow, as transcription and translation have to occur before any protein activity can be observed. Second, the method can be cumbersome to implement in mammalian cells, because additional factors may have to be introduced into the target cells. Third, a context-specific promoter is not readily generalizable.

An attractive strategy to circumvent the shortcomings of a promoter-based approach is to develop a Cas9 enzyme whose activity can be post-translationally controlled by an external input. Several laboratories have successfully engineered light-inducible systems based on Cas9 or transcription activator-like effectors (TALEs)[21–24]. However, specialized equipment that delivers blue light irradiation is currently uncommon, thereby restricting the adoption of such photoactivatable systems. A split Cas9 architecture has also been recently reported, whereby the Cas9 protein is divided into two fragments that can reassemble with the aid of rapamycin-binding dimerization domains to reconstitute the original enzymatic activity[25]. Although this system relies on a simple chemical input, it may be inconvenient to implement owing to the need to manipulate multiple Cas9 fragments. Another post-translational method that depends on the chemical-triggered excision of a function-disrupting intein has been shown to modulate the activity of Cas9 (ref. 16). However, this intein–Cas9 system is irreversible and cannot be switched off once the intein has been spliced out of the enzyme.

We sought an inducible genome-editing method that would have low background activity and a fast response time and would also be reversible, easy to implement, and widely applicable. Because the activity of the Cre recombinase can be regulated by tamoxifen or a related analog such as 4-HT when the enzyme is fused to a mutated ligand-binding domain of ERT2, we speculated that fusing ERT2 to Cas9 might also render the activity of the endonuclease dependent on the chemical (**Fig. 1a**). We demonstrated the feasibility of this strategy and, through a series of optimization steps, developed iCas, a Cas9 variant whose nuclease activity is tightly controlled by 4-HT. We further compared iCas with other chemical-inducible methods and showed that iCas had the fastest on rate and the highest editing efficiency upon induction while maintaining a reasonably low background activity without 4-HT. Additionally, we found that iCas can be switched on and off repeatedly, thereby opening up potential new applications that require continuous or periodic modulation of Cas9 function. Collectively, our results define a 'user-friendly' CRISPR–Cas9 platform for fast, reversible, chemical-inducible genome engineering in mammalian cells.

## RESULTS

### Initial development of a chemical-inducible Cas9 variant

We started by constructing and testing different fusions of the ERT2 domain with wild-type Cas9 derived from *Streptococcus pyogenes* (**Fig. 1b**). We placed ERT2 at either the N or C terminus of Cas9 and also varied the position of the nuclear localization signal (NLS). Using HEK293 cells, we evaluated the constructs for editing activity with and without 1 μM 4-HT by targeting four distinct genomic loci—a

[1]Genome Institute of Singapore, Agency for Science Technology and Research, Singapore. [2]School of Chemical and Biomedical Engineering, Nanyang Technological University, Singapore. [3]School of Biological Sciences, Nanyang Technological University, Singapore. [4]School of Life Sciences and Chemical Technology, Ngee Ann Polytechnic, Singapore. *e-mail: mh.tan@ntu.edu.sg

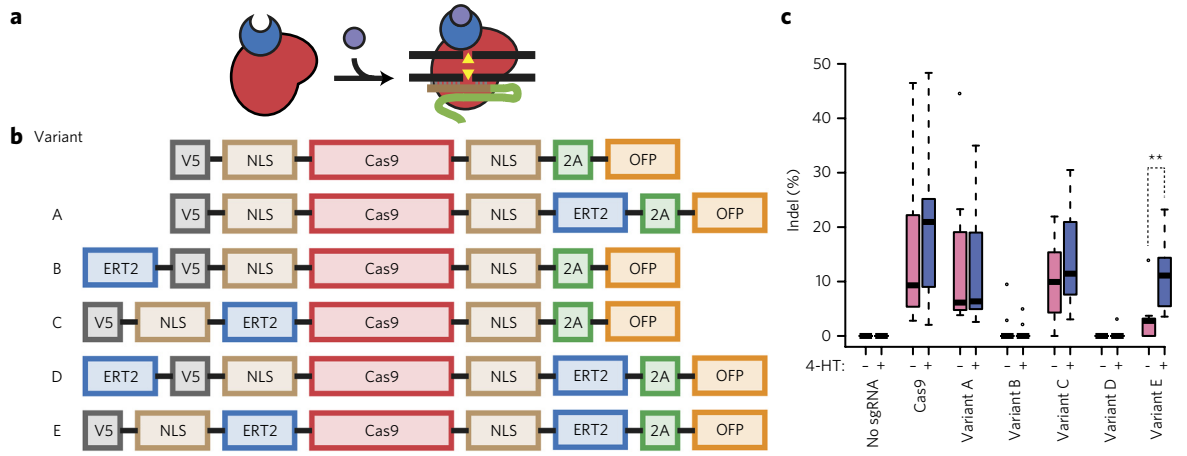



**Figure 1 | Building and testing a 4-HT-inducible Cas9.** (**a**) Schematic of the ERT2-based strategy. A fusion of Cas9 (red) and ERT2 (blue) was predicted to be sequestered in the cytoplasm. However, in the presence of an antagonist such as 4-HT (purple), the enzyme could enter the nucleus, form a complex with a sgRNA (brown and green), and generate a double-stranded break (yellow triangles) in the cell's DNA (black). (**b**) Architectures of different Cas9–ERT2 fusions tested. Top, the original wild-type Cas9 construct, which contains a V5 epitope tag and two NLSs joined to Cas9. The orange fluorescent protein (OFP) is separated from Cas9 by a 2A self-cleaving peptide. Other rows represent five distinct configurations of NLS, ERT2, and Cas9 that were evaluated in this study. (**c**) Extent of genome modification determined by the Surveyor cleavage assay. Four genomic loci were tested, with each locus evaluated in at least two biological replicates, giving a total of eight independent experiments. Boxplots indicate the range of indels obtained from all the experiments. Wild-type Cas9 generated robust DNA modifications at all the targeted loci with or without 4-HT. In contrast, variant E, an ERT2–Cas9–ERT2 fusion, exhibited low activity in the absence of 4-HT but significantly higher activity in the presence of the chemical (**$P < 0.05$, Student's $t$-test).

© 2016 Nature America, Inc. All rights reserved.

coding exon of the gene *EMX1*, an intron of *PPP1R12C*, and two separate sites in the promoter of *VEGFA*. From a Surveyor assay, we found that only variant E, an ERT2–Cas9–ERT2 fusion, showed low editing activity without 4-HT and significantly higher activity when the chemical was added ($P < 0.05$, Student's $t$-test) across all four targeted loci (**Fig. 1c**). We further confirmed the results by Illumina deep sequencing (**Supplementary Results**, **Supplementary Fig. 1a**) and by Sanger sequencing of individual clones (**Supplementary Fig. 1b**). The difference in genome-editing activity with and without 4-HT was not due to a change in overall Cas9 protein abundance but rather to a dramatic change in the amount of Cas9 present in the nucleus (**Supplementary Fig. 2**). Collectively, our data indicated that fusion of ERT2 domains to both the N and C termini of Cas9 rendered the endonuclease activity of Cas9 dependent on 4-HT by sequestering the enzyme in the cytoplasm in the absence of the inducer; upon addition of 4-HT, the ERT2–Cas9–ERT2 protein was able to translocate into the nucleus to perform its function.

## Optimization of the ERT2-Cas9-ERT2 architecture

Though our preliminary results were promising, all the initial fusion variants showed some background activity without 4-HT. We thus sought to improve our conditional genome-editing system. First, we varied the lengths and amino acid compositions of the protein linkers between each ERT2 domain and the Cas9 enzyme. We tested linker lengths that ranged from 2 to 20 aa and focused the linker composition primarily on six amino acids (A, E, G, P, S, and T) that had been reported to be ideal for generating open flexible loops[26]. Second, because the size of Cas9 is around four times that of Cre (160 kDa versus 40 kDa), we reasoned that more copies of the ERT2 domain may be required to fully control the cellular localization and subsequent activity of Cas9. Thus, we tested different copy numbers of ERT2 at either the N or C terminus of the endonuclease. In total, we constructed 30 variants with distinct configurations for further analysis (**Fig. 2a** and **Supplementary Table 1**). We classified the variants into four groups on the basis of how they differed from the initial ERT2–Cas9–ERT2 fusion.

To assay the activities of the Cas9 variants, we employed a previously described GFP disruption assay[4] (**Supplementary Fig. 3**). We used two different sgRNAs to target nonoverlapping regions of the gene encoding GFP. For comparison, we included the original ERT2–Cas9–ERT2 fusion (variant E) and the wild-type Cas9 enzyme, which provided an estimation of the maximum possible reduction in fluorescence signal. As we expected, cells transfected with wild-type Cas9 showed a high reduction in GFP intensity regardless of whether 4-HT was present (**Fig. 2b**). In contrast, all the variants tested showed greater loss of GFP expression upon 24 h of 4-HT treatment (**Supplementary Fig. 4a**). Notably, most of the variants also showed some loss of fluorescence signal even without 4-HT, suggesting activity leakage. The variants that showed the least leakage belonged to groups 3 and 4, which contained two copies of ERT2 on the C terminus of Cas9.

To confirm the results from our GFP disruption experiments, we performed a Surveyor assay to detect genome modifications (**Fig. 2c** and **Supplementary Fig. 4b**) and also analyzed the mutation landscape by Illumina deep sequencing (**Supplementary Figs. 4c** and **5**) using *EMX1* as a test genomic locus. Consistently, we found that varying the linker length or composition alone generally did not improve the performance of our inducible system. Instead, increasing the copy number of ERT2 domains, particularly on the C terminus of Cas9, resulted in an overall level of background activity that was not significantly different from the no-sgRNA control. Notably, the fusion of additional ERT2 domains did not inactivate Cas9, as all the variants tested gave more insertions and deletions (indels) upon 4-HT treatment (1 μM).

We next examined all the data together to identify the best-performing variants. The rank orders of the Cas9 variants in at least two out of the three assays agreed well with one another ($P < 0.05$, Kolmogorov–Smirnov test) (**Supplementary Fig. 6**). Notably, 8 out of the 30 Cas9 variants demonstrated a consistently lower level of background activity than the original ERT2–Cas9–ERT2 fusion (variant E) across all experiments (**Supplementary Fig. 7**). However, only three of these (variants 27, 29, and 30), all of which were from group 4, showed consistent and robust editing activity upon induction (**Fig. 2d**). Hence, we pursued variants 27, 29, and 30 further, as they gave a high percentage of genome modifications with 4-HT but a low percentage of indels without the chemical.

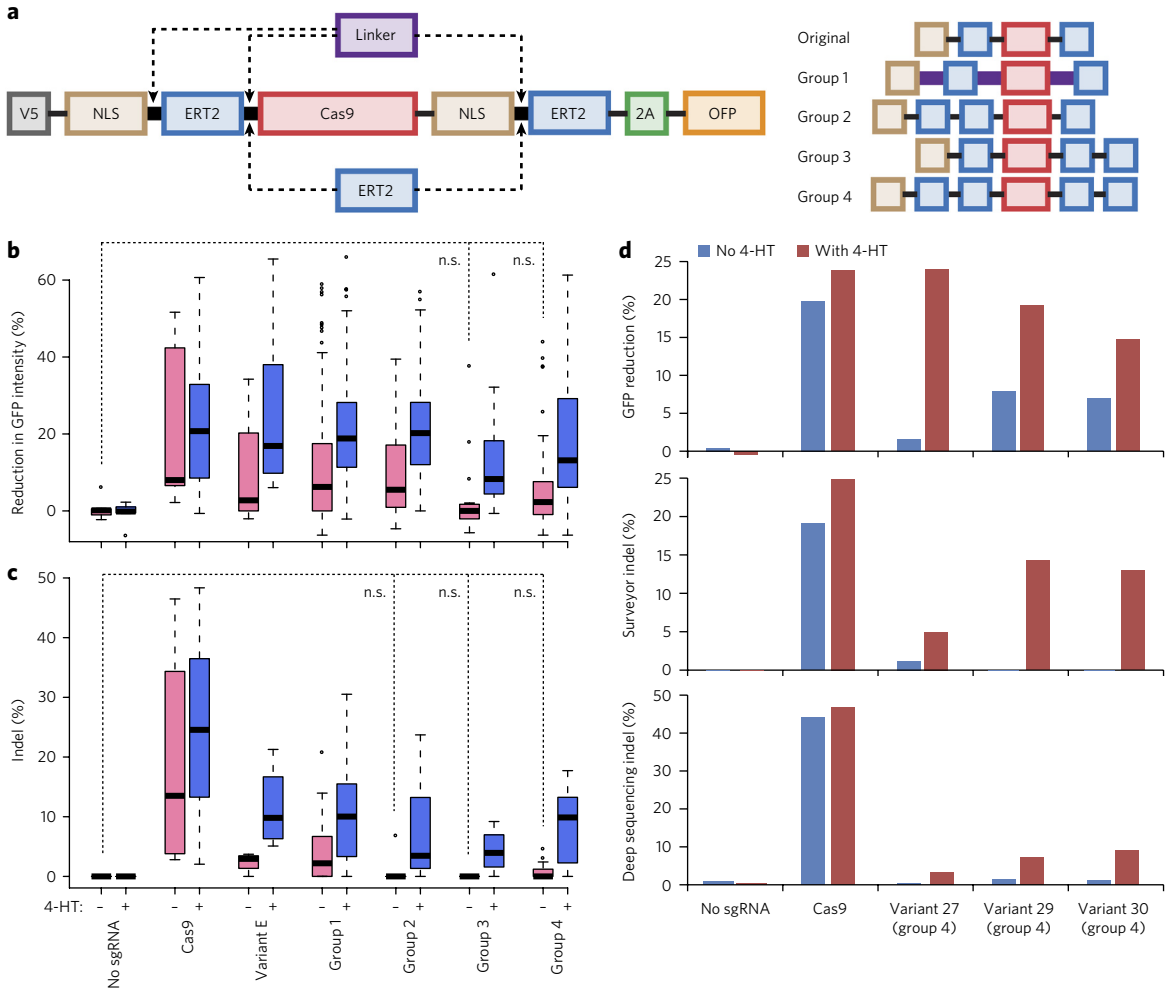



**Figure 2 | Optimization of the ERT2–Cas9–ERT2 architecture.** (**a**) Left, placement of linkers and ERT2 copies evaluated in this study. Right, grouping of the 30 Cas9 variants tested on the basis of how they differ from the original variant E (see **Supplementary Table 1** for details). OFP, orange fluorescent protein; 2A, self-cleaving peptide. (**b**) GFP disruption activity of the 30 Cas9 variants, wild-type Cas9, and the original variant E in the absence or presence of 4-HT. Boxes represent the range of values achieved by every variant within a particular group. Center lines, median; box limits, interquartile range; whiskers, 1.5× interquartile range. Each construct was tested in at least six biological replicates. n.s., not significant ($P > 0.25$, Wilcoxon rank-sum test). (**c**) Detection of genome modification by Surveyor assay. Target site DNA was amplified from cells transfected with wild-type Cas9 or a Cas9 variant and treated with or without 4-HT ($n = 2$ biological replicates per construct). n.s., not significant ($P > 0.25$, Wilcoxon rank-sum test). (**d**) GPF reduction and indel percentages for the best-performing Cas9 variants. Each variant contained four copies of ERT2 and showed 4-HT-dependent activity, as assessed by GFP disruption assay (top), Surveyor assay (middle), and deep sequencing experiments (bottom). Transfection of wild-type Cas9 without and with the appropriate sgRNA served as negative and positive control, respectively.

## Performance of iCas under various 4-HT treatment regimes

As the amount of active Cas9 in the cell should be tightly controlled[12,15,16], we sought to ascertain the behavior of our optimized Cas9 variants under various treatment conditions. We tested three concentrations of 4-HT (10 nM, 100 nM, and 1000 nM) and six durations of chemical treatment (2 h, 4 h, 6 h, 8 h, 16 h, 24 h, and 48 h) for variants 27, 29, and 30. We quantified genome modification at the *EMX1* locus using the Surveyor assay (**Supplementary Fig. 8a**). Cleavage activity was detected within 4 h of 4-HT treatment for all three variants and showed an increasing trend with longer treatment durations, which we further confirmed by deep sequencing (**Supplementary Fig. 8b**). Notably, owing to its higher sensitivity, deep sequencing also revealed a low level of DNA editing after just 2 h of 4-HT treatment. Additionally, we found that 4-HT yielded a significantly lower level of nuclease activity at 10 nM than at 100 nM or 1,000 nM ($P < 0.005$, Wilcoxon rank-sum test) (**Supplementary Fig. 9**). Hence, we used either 100 nM or 1,000 nM 4-HT in all subsequent experiments.

A key performance measure of an inducible system is whether the system exhibits any background activity. The Surveyor assay showed low amount of genome modification at the *EMX1* locus for all three variants without 4-HT, although cleavage was observed only at the last time point (48 h) for variant 30 (**Supplementary Fig. 8a**). From deep sequencing, leaky activity was first detected at 6 h, 2 h, and 16 h for variants 27, 29, and 30, respectively (**Supplementary Fig. 8b**). Subsequently, we tested whether the three variants displayed leaky activity at six other endogenous genomic loci, namely two sites in the promoter of *VEGFA*, two sites in an intron of *WAS*, one site in an intron of *TAT*, and one site in a coding exon of *FANCF*. Genomic DNA was isolated 24 h after transfection without 4-HT treatment and analyzed by the Surveyor assay (**Fig. 3a**). Consistent with our *EMX1* results, we observed a low amount of genome modification at four loci for variant 27 and at two loci for variant 29. No cleavage bands were detected for variant 30. Additionally, the leakiness in activity observed for variants 27 and 29 became more pronounced over time (**Supplementary Fig. 10**).

© 2016 Nature America, Inc. All rights reserved.

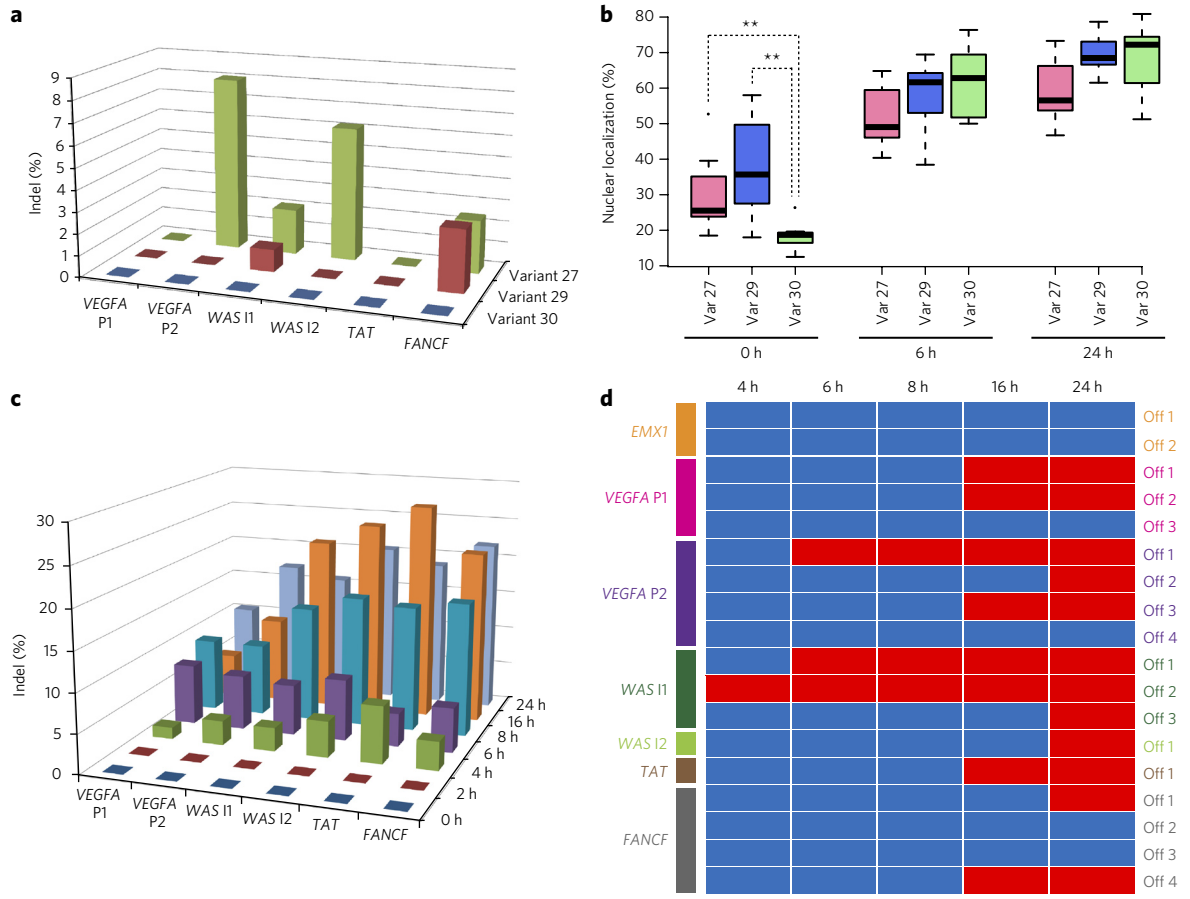



**Figure 3 | Optimization of 4-HT treatment conditions.** (**a**) Background activity of Cas9 variants 27, 29, and 30 at multiple genomic loci (P1 and P2, promoter sites; I1 and I2, intron sites), as determined by Surveyor assay to quantify indel frequency ($n = 1$ replicate for variants 27 and 29; $n = 2$ (*VEGFA* P1 and P2) or 3 (*WAS* I1 and I2, *TAT*, and *FANCF*) biological replicates for variant 30). (**b**) Intracellular localization of the Cas9 variants as determined by immunohistochemistry. Transfected HEK293 cells were untreated (0 h) or treated with 4-HT for 6 or 24 h before they were fixed and stained ($n = 7$ biological replicates per construct and time point). At least 300 cells were counted for each sample. Although 4-HT treatment led to an increase in the percentage of cells containing nuclear protein for all three Cas9 constructs, variant 30 showed the lowest percentage of cells with nuclear Cas9 in the absence of 4-HT (**$P < 0.05$, Wilcoxon rank-sum test); var, variant. Center lines, median; box limits, interquartile range; whiskers, 1.5× interquartile range. (**c**) Targeting efficiency of iCas (variant 30) across multiple genomic loci. Cells were analyzed by Surveyor assay after different durations of treatment with 1 μM 4-HT, applied 24 h after transfection ($n \geq 2$ biological replicates for each locus and time point; see Online Methods for details). (**d**) DNA-modification specificity of iCas with different durations of 4-HT treatment, analyzed by Surveyor assay for off-target modifications (off) at various loci. Blue indicates no cleavage observed; red indicates the presence of cleavage bands (see **Supplementary Table 2** for details).

To verify the results from our Surveyor assays and deep sequencing experiments, we performed immunohistochemical staining to determine the subcellular localization of the three variants, all of which contained two copies of ERT2 at both termini of the enzyme ($(ERT2)_2$–Cas9–$(ERT2)_2$), with or without 1 μM 4-HT. Twenty-four hours after transfection with plasmids carrying a Cas9 variant and a sgRNA targeting the *EMX1*, *VEGFA*, *FANCF*, *WAS*, or *TAT* genomic locus, the cells were either fixed immediately and stained with anti-V5 or were subjected to 6 h or 24 h 4-HT treatment before fixation and staining (**Supplementary Fig. 11**). We quantified the percentage of cells that showed a nuclear localization of $(ERT2)_2$–Cas9–$(ERT2)_2$ (**Fig. 3b**). For all three Cas9 variants, we observed that addition of 4-HT led to a significant increase in the percentages of cells exhibiting a nuclear localization of $(ERT2)_2$–Cas9–$(ERT2)_2$ ($P < 0.05$, Student's *t*-test). Most of the protein translocation occurred within the first 6 h of 4-HT treatment. Importantly, in the absence of 4-HT, cells that were transfected with variant 30 showed significantly less nuclear localization of $(ERT2)_2$–Cas9–$(ERT2)_2$ than cells that were transfected with variant 27 or variant 29 ($P < 0.05$, Student's *t*-test). Collectively, these data indicated that variant 30 had less background activity than variants 27 and 29 across multiple loci, thereby suggesting that variant 30 could be used for precise control of genome editing. Hence, all subsequent experiments were performed with variant 30, hereafter referred to as iCas.

We sought to test the robustness of iCas by using it to target the *VEGFA* promoter as well as the *WAS*, *TAT*, and *FANCF* genes for different durations of 1 μM 4-HT treatment (2 h, 4 h, 6 h, 8 h, 16 h, and 24 h). Consistently, the Surveyor assay showed nuclease activity within 4 h of 4-HT treatment for all loci tested (**Fig. 3c**). The editing activity continued to increase with longer treatment durations. Additionally, iCas showed similarly fast responses to 4-HT in different human cell lines (**Supplementary Fig. 12**). These results indicate that iCas is a robust inducible genome-editing system in mammalian cells.

## Specificity of iCas at endogenous off-target sites

To assess the DNA cleavage specificity of iCas, we measured the modification of known Cas9 off-target sites of the *EMX1*, *VEGFA*, *FANCF*, *WAS*, and *TAT* sgRNAs[27–29]. Twenty-four hours after transfection, we treated HEK293 cells with 1 μM 4-HT for different durations

© 2016 Nature America, Inc. All rights reserved.

(4 h, 6 h, 8 h, 16 h, or 24 h) and used the Surveyor assay to assess editing activity at each off-target site (**Fig. 3d** and **Supplementary Fig. 13**). Overall, cleavage at off-target sites tended to emerge later than at the corresponding on-target sites, or it occurred at lower levels, which we further confirmed by deep sequencing (**Supplementary Fig. 14**). Nevertheless, the sgRNAs tested could be divided into three groups. In the first group, the sgRNAs were highly specific for their intended target (**Supplementary Figs. 13a** and **14a**). For *EMX1*, our iCas system did not yield any measurable cleavage at the two off-target sites tested, but wild-type Cas9 produced off-target modifications as described previously[28,29] (**Supplementary Fig. 15**). In the second group, the sgRNAs were moderately specific, as exemplified by the *TAT* sgRNA (**Supplementary Figs. 13b** and **14b**). Here, the optimal time window of 4-HT treatment for minimizing off-target effects appeared to be around 4–8 h. In the third group, the sgRNAs were unspecific, and genome modifications could be detected at on-target and off-target sites at approximately the same time (**Supplementary Figs. 13c** and **14c**). For these sgRNAs, we were unable to tune the duration of chemical treatment to obtain the desired target genome modification without considerable off-target editing. Collectively, our data showed that limiting Cas9 activity is generally a viable strategy to improve the specificity of the endonuclease at most but not all genomic loci.

## Comparison of iCas with a promoter-based approach

As different methods may be adopted for inducible genome editing, we compared iCas with an alternative strategy whereby the wild-type Cas9 enzyme was expressed under a doxycycline (dox)-inducible promoter ($P_{TRE3G}$-Cas9). To this end, we used a previously reported STF3A cell line[30–32] that carries a Wnt-responsive luciferase reporter and also strongly expresses a Wnt ligand, thereby giving high reporter activity. We reasoned that if β-catenin, a key signal transducer in the Wnt pathway, was inactivated, luciferase expression would be reduced considerably. We thus sought to use iCas or $P_{TRE3G}$-Cas9 to knock out *CTNNB1*, which encodes β-catenin, and to determine how rapidly each conditional system could perturb Wnt signaling upon induction.

We first stably integrated a gene encoding the Tet-On 3G transactivator, which binds to and activates expression from $P_{TRE3G}$ in the presence of dox, into the STF3A cell line (**Supplementary Fig. 16a**) and verified the functionality of the engineered (STF3A-Tet-On) cells (**Supplementary Fig. 16b**). Next, we used iCas or $P_{TRE3G}$-Cas9 to target the second coding exon of *CTNNB1* near the ATG start codon. Twenty-four hours after transfection, we treated cells with 1 μM 4-HT or 1 μg/ml dox for 6 h, 12 h, or 24 h and then harvested the cells for analysis by Surveyor assay. iCas was consistently able to modify the target locus within 6 h of 4-HT treatment, and the indel frequency increased with longer exposures to 4-HT (**Fig. 4a**). No cleavage bands were observed in the absence of 4-HT at any time point. However, for the $P_{TRE3G}$–Cas9 system, cleavage bands were only observed after the cells were exposed to dox for 24 h.

To demonstrate the impact of genome modification at the *CTNNB1* locus, we performed luciferase assays on the STF3A-Tet-On cell line after transfection with iCas or $P_{TRE3G}$-Cas9. Cells were treated for 6 h with the corresponding chemical and then harvested after another 72 h to allow sufficient time for changes in β-catenin or luciferase protein levels. We verified that both the transcript and protein levels of β-catenin were downregulated in cells cotransfected with iCas and an *CTNNB1*-targeting sgRNA (**Supplementary Fig. 17**). Consequently, we observed a significant decrease in luciferase activity in these cells ($P < 0.001$, Student's *t*-test) (**Fig. 4b**). In contrast, there was no significant change in β-catenin expression or luciferase activity in cells transfected with an *EMX1*-targeting sgRNA or $P_{TRE3G}$-Cas9. Additionally, the expression profiles of known Wnt target genes paralleled the results from our luciferase assays (**Fig. 4c** and **Supplementary Fig. 18**).

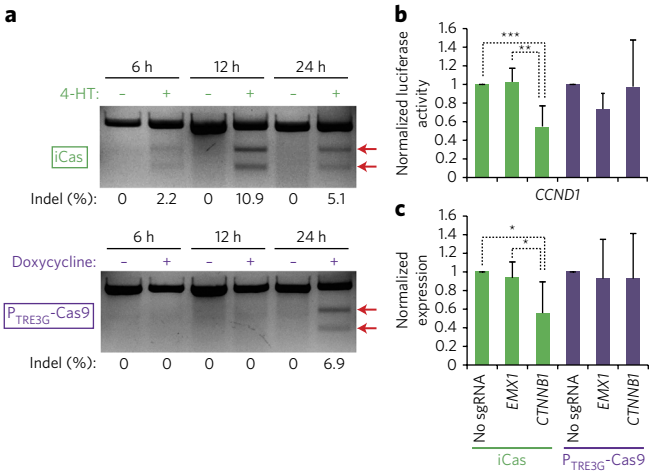



**Figure 4 | Comparison of iCas with an alternative inducible-promoter-based system.** (**a**) Detection of genome modification at the *CTNNB1* locus by Surveyor assay. Red arrows indicate the expected cleavage bands. The full gel image is shown in **Supplementary Figure 24**. (**b**) Repression of Wnt signaling pathway assayed by a Wnt-responsive luciferase reporter. A plasmid encoding either iCas (green) or $P_{TRE3G}$-Cas9 (purple) was transfected into STF3A-Tet-On cells with or without sgRNA. The transfected cells were treated with 4-HT or dox for 6 h and harvested after another 72 h. All luciferase readings were normalized to those from control samples (no sgRNA). Data represent mean ± s.d. of 5 biological replicates (**$P < 0.005$, ***$P < 0.001$, Student's *t*-test). (**c**) Expression of *CCND1*, a Wnt target gene, measured by quantitative real-time PCR. Data represent mean ± s.d. of 5 biological replicates (*$P < 0.05$, Student's *t*-test).

Collectively, these data highlight the iCas system's advantage in speed over an alternative inducible-promoter approach in temporal control of genome-editing activity.

## Benchmarking different post-translational control systems

Two other chemical-inducible strategies that rely on post-translational control were recently reported[16,25], and we sought to benchmark iCas against them. We cloned the best-performing intein–Cas9 and split-Cas9 constructs from these studies into the same plasmid backbone as iCas and performed all experiments side by side in HEK293 cells to ensure a fair comparison. We induced the iCas and intein–Cas9 systems with 1 μM 4-HT and the split-Cas9 system with 200 nM rapamycin, on the basis of the published reports[16,25].

For the comparison, we targeted the *EMX1*, *TAT*, and *WAS* genomic loci with or without the appropriate inducer. Different durations of chemical treatment were tested, and the extent of genome modification was measured by the Surveyor assay (**Fig. 5a** and **Supplementary Fig. 19a**) and by deep sequencing (**Supplementary Fig. 20a**). Overall, without the inducer, the split-Cas9 architecture showed the lowest level of background activity, and iCas and intein–Cas9 had comparable levels of leakiness. However, with the inducer, iCas consistently showed higher cleavage efficiency than intein–Cas9 and split-Cas9, at all time points and genomic loci. Notably, the amount of indels produced by active iCas was 1.6- to 4.8-fold higher than those produced by the reassembled split-Cas9 complex. Hence, the lower background observed in split-Cas9 appeared to be a consequence of an overall reduction in editing activity.

Next, we calculated the switching ratio, which we define as the extent of genome modification with the relevant inducer divided by the extent of genome modification without the inducer (**Fig. 5b** and **Supplementary Figs. 19b** and **20b**). Overall, the iCas system and the split-Cas9 architecture produced similar switching ratios. However, in the Surveyor assay, iCas showed significantly higher ratios than

© 2016 Nature America, Inc. All rights reserved.

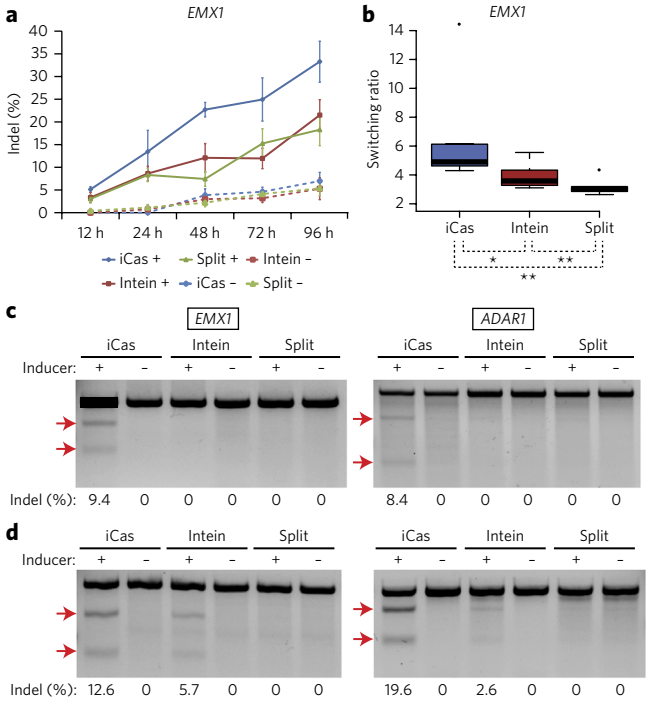



**Figure 5 | Comparison of iCas with intein–Cas9 and split-Cas9.** (**a**) Detection of genome modification at the *EMX1* locus by Surveyor cleavage assay. Transfected HEK293 cells were treated with (+, solid lines) or without (–, dashed lines) chemical inducer and harvested at 12, 24, 48, 72, or 96 h after treatment. Data represent mean ± s.e.m. of 4 (12, 24, 48, and 96 h) or 8 (72 h) biological replicates. (**b**) Switching ratios at the *EMX1* locus upon addition of inducer. $^{*}P < 0.1$, $^{**}P < 0.05$, Student's *t*-test. Center lines, median; box limits, interquartile range; whiskers, 1.5× interquartile range. (**c**,**d**) Surveyor cleavage assay evaluating the ability of iCas, intein–Cas9, and split-Cas9 to edit two genomic loci simultaneously after 12 (**c**) or 24 h (**d**) of inducer treatment. Red arrows indicate the expected cleavage bands. (Full gel images are shown in **Supplementary Fig. 25**.)

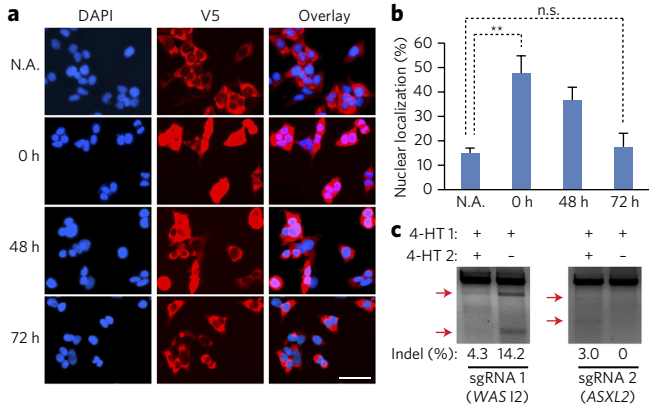



**Figure 6 | Toggling the activity of iCas on and off.** (**a**,**b**) Immunofluorescence images (**a**) and quantification (**b**) of iCas in HEK293-iCas cells either untreated (N.A.) or treated with 4-HT and then fixed at 0, 48, or 72 h after removal of 4-HT from the culture medium. DAPI, nuclear staining; V5, antibody specific for V5-tagged Cas9. Scale bar, 50 µm. In **b**, at least 300 cells were counted for each sample and time point. Data represent mean ± s.d. from three biological replicates. n.s., not significant ($P > 0.25$); $^{**}P < 0.001$, Student's *t*-test. (**c**) Surveyor assay detection of genome modification in HEK293 cells after two cycles of transfection and 4-HT treatment (4-HT 1 and 4-HT 2). A sgRNA targeting the *WAS* locus was transfected first, and a sgRNA targeting the *ASXL2* locus second. Red arrows indicate the expected cleavage bands. (The full gel image is shown in **Supplementary Fig. 26**.)

intein–Cas9 at the *EMX1* and *WAS* loci ($P < 0.1$, Student's *t*-test), and in deep sequencing it showed significantly higher switching ratios than intein–Cas9 at all tested loci ($P < 0.05$, Student's *t*-test). These results suggest that iCas is turned on more efficiently than intein–Cas9 upon addition of 4-HT.

Besides single gene targeting, we compared the ability of iCas to perform multiplex genome engineering with that of intein–Cas9 or split-Cas9. We cotransfected HEK293 cells with a sgRNA targeting *EMX1* and another sgRNA targeting a coding exon of *ADAR1* (*ADAR*) and analyzed the extent of genome modification by the Surveyor assay. After 12 h of chemical treatment, we observed that iCas generated indels at both the *EMX1* and *ADAR1* genomic loci (**Fig. 5c**). In contrast, intein–Cas9 and split-Cas9 did not produce detectable cleavage at any of the targeted locus. Additionally, after 24 h of chemical treatment, iCas produced more genome modification than at 12 h, and intein–Cas9 was also able to edit both the *EMX1* and *ADAR1* loci (**Fig. 5d**). However, split-Cas9 still did not edit any of the targeted genes. We further confirmed these results with a different pair of sgRNAs (**Supplementary Fig. 20c**). Collectively, our data highlight the advantage of iCas over intein–Cas9 and split-Cas9 in performing conditional multiplex genome editing.

## Repeated toggling of iCas activity

In principle, a conditional system such as iCas should allow users to generate stable cell lines and induce its activity whenever needed. To demonstrate this, we used retroviral transduction to establish a HEK293 cell line that stably expresses iCas (HEK293-iCas cells). We verified that the cell line was functional (**Supplementary Fig. 21a**) and monitored the intracellular localization of iCas by immunofluorescence (**Fig. 6a**). Without 4-HT, most cells produced iCas protein that was localized in the cytoplasm; only 15% of the cells contained nuclear-localized protein. However, upon 24 h treatment with 4-HT, the proportion of cells with nuclear-localized protein increased significantly, to 48% ($P < 0.001$, Student's *t*-test). We then washed away the inducer and immunostained the cells with anti-V5 at 48 and 72 h after removal of 4-HT. Quantification of microscopy images showed that by 72 h, the percentage of cells with nuclear-localized protein had decreased to a level that was not significantly different from that of the preinduction state (**Fig. 6b**).

Subsequently, we explored the possibility of toggling the activity of iCas (**Supplementary Fig. 21b**). After 1 µM 4-HT treatment of HEK293 cells cotransfected with iCas and a first sgRNA targeting the *WAS* locus, we removed the inducer and waited 72 h to allow nuclear-localized iCas protein to exit the nucleus before introducing a second sgRNA targeting a coding exon of *ASXL2*. The cells were then either treated with 4-HT a second time or left untreated. From the Surveyor assay, cleavage activity was readily observed at both targeted loci for cells that were treated twice with the inducer (**Fig. 6c**); however, cleavage was detected only at the *WAS* locus in cells that were exposed to 4-HT after the first transfection but not after the second transfection, indicating that iCas was successfully switched off after the first induction event. Hence, our results indicate that iCas is a reversible genome-editing system.

## DISCUSSION

We have developed iCas, an optimized $(ERT2)_2$–Cas9–$(ERT2)_2$ fusion protein, that allows tight spatiotemporal control of genome modification using a chemical input. The ERT2 domains effectively sequester Cas9 outside the nucleus, where it cannot perform its DNA-editing activity. In the presence of 4-HT, however, the fusion protein translocates rapidly into the nucleus to perform its function.

© 2016 Nature America, Inc. All rights reserved.

During the development process, we observed that there was, in general, a compromise between targeting efficiency and leakiness in editing activity. As we sought to minimize the background activity of our fusion protein, we observed a concomitant decline in the efficiency of the endonuclease even with 4-HT. Nevertheless, through fusing additional ERT2 domains for tighter regulation and adjusting the different linker lengths, we managed to reduce background activity to a minimum while retaining around 38–60% of the original wild-type Cas9 activity in the presence of 4-HT.

A key issue in the application of CRISPR–Cas9 technology to genome engineering is the specificity of the endonuclease. Different strategies have been developed to enhance the specificity of DNA editing with Cas9 (refs. 4–16). One attractive approach is to limit the dosage of the active enzyme so that there will be enough to modify the intended on-target genomic locus but an insufficient amount to cleave potential off-target sites. Here we assessed the feasibility of such an approach and found that iCas had improved specificity over wild-type Cas9 for most of the sgRNAs tested when we limited the duration of 4-HT treatment to 4–8 h. However, for two of the sgRNAs tested, modification of off-target and on-target sites occurred at around the same time. This might be because the sgRNAs have similar affinities for the on-target and off-target sites. Notably, previous studies on global profiling of DNA double-stranded breaks induced by CRISPR–Cas9 have reported that for some sgRNAs, the preferred site is not the intended on-target locus but an alternative site with one or more mismatches to the target sequence[27,28]. Hence, it appears that the substrate selectivity of the Cas9 endonuclease is still not fully understood.

Because different methods for conditional genome engineering exist, we compared the performance of iCas with three other chemical-inducible approaches. iCas showed a substantial advantage in speed of response over $P_{TRE3G}$-Cas9. Unexpectedly, however, iCas also showed a consistently faster on rate and higher cleavage efficiency upon induction than both split-Cas9 and intein–Cas9 (refs.16,25) across multiple genomic loci. Nevertheless, the biggest weakness of iCas is its background activity, which is typically higher than that of the split-Cas9 architecture. A potential solution to alleviate the problem is to reduce the dosage of iCas. No background activity was detected by the Surveyor assay in our HEK293-iCas stable cell line (**Supplementary Fig. 21a**), possibly owing to a lower expression of iCas in these cells than in the plasmid-transfected cells used in our evaluation studies (**Supplementary Fig. 22**). Transfection of lower amounts of iCas plasmid also led to a decrease in leaky cutting (**Supplementary Fig. 23**). However, because of the trade-off between potency and leakiness, further work is needed to determine the precise dosage of iCas that is high enough for satisfactory gene editing with 4-HT but low enough to minimize background activity.

Conditional genome-engineering methodologies have wide applicability in many areas of basic and translational research. For example, inducible systems can be used to investigate embryonic development or stem cell differentiation. iCas can be used to dissect the function of a gene in a late developmental stage or in a terminally differentiated cell type when the gene is also essential earlier in development or in pluripotent stem cells. In some cases, the timing of genetic perturbation can be critical. For example, during *Xenopus* development, zygotic gene activation occurs within 6 h of fertilization, and other important events, such as gastrulation and neurulation, are completed in less than 10 h. As large changes in gene expression can occur within a short period of time[33], a fast-responding inducible system is required to dissect the dynamic regulatory network orchestrating vertebrate development.

In conclusion, we have developed a conditional genome-editing system that is rapidly inducible, shows high cleavage efficiency upon induction but reasonably low background activity without 4-HT, can target multiple genomic loci simultaneously, and is reversible. The fast response time will enable applications that demand tight temporal control. For spatial control, one may apply photocaged tamoxifen or 4-HT and use ultraviolet light to target a subset of cells within a mixed population[34]. Hence, our ERT2-based iCas technology expands the toolkit for precise genome engineering in mammalian cells.

Received 16 February 2016; accepted 13 July 2016;
published online 12 September 2016

## METHODS

Methods and any associated references are available in the online version of the paper.

## References

1. Cho, S.W., Kim, S., Kim, J.M. & Kim, J.S. Targeted genome engineering in human cells with the Cas9 RNA-guided endonuclease. *Nat. Biotechnol.* **31**, 230–232 (2013).
2. Cong, L. *et al.* Multiplex genome engineering using CRISPR/Cas systems. *Science* **339**, 819–823 (2013).
3. Mali, P. *et al.* RNA-guided human genome engineering via Cas9. *Science* **339**, 823–826 (2013).
4. Guilinger, J.P., Thompson, D.B. & Liu, D.R. Fusion of catalytically inactive Cas9 to FokI nuclease improves the specificity of genome modification. *Nat. Biotechnol.* **32**, 577–582 (2014).
5. Ran, F.A. *et al.* Double nicking by RNA-guided CRISPR Cas9 for enhanced genome editing specificity. *Cell* **154**, 1380–1389 (2013).
6. Shen, B. *et al.* Efficient genome modification by CRISPR-Cas9 nickase with minimal off-target effects. *Nat. Methods* **11**, 399–402 (2014).
7. Tsai, S.Q. *et al.* Dimeric CRISPR RNA-guided FokI nucleases for highly specific genome editing. *Nat. Biotechnol.* **32**, 569–576 (2014).
8. Mali, P. *et al.* CAS9 transcriptional activators for target specificity screening and paired nickases for cooperative genome engineering. *Nat. Biotechnol.* **31**, 833–838 (2013).
9. Fu, Y., Sander, J.D., Reyon, D., Cascio, V.M. & Joung, J.K. Improving CRISPR-Cas nuclease specificity using truncated guide RNAs. *Nat. Biotechnol.* **32**, 279–284 (2014).
10. Kleinstiver, B.P. *et al.* High-fidelity CRISPR-Cas9 nucleases with no detectable genome-wide off-target effects. *Nature* **529**, 490–495 (2016).
11. Slaymaker, I.M. *et al.* Rationally engineered Cas9 nucleases with improved specificity. *Science* **351**, 84–88 (2016).
12. Kim, S., Kim, D., Cho, S.W., Kim, J. & Kim, J.S. Highly efficient RNA-guided genome editing in human cells via delivery of purified Cas9 ribonucleoproteins. *Genome Res.* **24**, 1012–1019 (2014).
13. Ramakrishna, S. *et al.* Gene disruption by cell-penetrating peptide-mediated delivery of Cas9 protein and guide RNA. *Genome Res.* **24**, 1020–1027 (2014).
14. Lin, S., Staahl, B.T., Alla, R.K. & Doudna, J.A. Enhanced homology-directed human genome engineering by controlled timing of CRISPR/Cas9 delivery. *eLife* **3**, e04766 (2014).
15. Zuris, J.A. *et al.* Cationic lipid-mediated delivery of proteins enables efficient protein-based genome editing *in vitro* and *in vivo*. *Nat. Biotechnol.* **33**, 73–80 (2015).
16. Davis, K.M., Pattanayak, V., Thompson, D.B., Zuris, J.A. & Liu, D.R. Small molecule-triggered Cas9 protein with improved genome-editing specificity. *Nat. Chem. Biol.* **11**, 316–318 (2015).
17. Shen, Z. *et al.* Conditional knockouts generated by engineered CRISPR-Cas9 endonuclease reveal the roles of coronin in *C. elegans* neural development. *Dev. Cell* **30**, 625–636 (2014).
18. Dow, L.E. *et al.* Inducible in vivo genome editing with CRISPR-Cas9. *Nat. Biotechnol.* **33**, 390–394 (2015).
19. González, F. *et al.* An iCRISPR platform for rapid, multiplexable, and inducible genome editing in human pluripotent stem cells. *Cell Stem Cell* **15**, 215–226 (2014).
20. Wang, T., Wei, J.J., Sabatini, D.M. & Lander, E.S. Genetic screens in human cells using the CRISPR-Cas9 system. *Science* **343**, 80–84 (2014).
21. Konermann, S. *et al.* Optical control of mammalian endogenous transcription and epigenetic states. *Nature* **500**, 472–476 (2013).
22. Polstein, L.R. & Gersbach, C.A. A light-inducible CRISPR-Cas9 system for control of endogenous gene activation. *Nat. Chem. Biol.* **11**, 198–200 (2015).
23. Nihongaki, Y., Yamamoto, S., Kawano, F., Suzuki, H. & Sato, M. CRISPR-Cas9-based photoactivatable transcription system. *Chem. Biol.* **22**, 169–174 (2015).
24. Nihongaki, Y., Kawano, F., Nakajima, T. & Sato, M. Photoactivatable CRISPR-Cas9 for optogenetic genome editing. *Nat. Biotechnol.* **33**, 755–760 (2015).
25. Zetsche, B., Volz, S.E. & Zhang, F. A split-Cas9 architecture for inducible genome editing and transcription modulation. *Nat. Biotechnol.* **33**, 139–142 (2015).

© 2016 Nature America, Inc. All rights reserved.

26. Schellenberger, V. *et al.* A recombinant polypeptide extends the *in vivo* half-life of peptides and proteins in a tunable manner. *Nat. Biotechnol.* **27**, 1186–1190 (2009).
27. Wang, X. *et al.* Unbiased detection of off-target cleavage by CRISPR-Cas9 and TALENs using integrase-defective lentiviral vectors. *Nat. Biotechnol.* **33**, 175–178 (2015).
28. Tsai, S.Q. *et al.* GUIDE-seq enables genome-wide profiling of off-target cleavage by CRISPR-Cas nucleases. *Nat. Biotechnol.* **33**, 187–197 (2015).
29. Fu, Y. *et al.* High-frequency off-target mutagenesis induced by CRISPR-Cas nucleases in human cells. *Nat. Biotechnol.* **31**, 822–826 (2013).
30. Xu, Q. *et al.* Vascular development in the retina and inner ear: control by Norrin and Frizzled-4, a high-affinity ligand-receptor pair. *Cell* **116**, 883–895 (2004).
31. Coombs, G.S. *et al.* WLS-dependent secretion of WNT3A requires Ser209 acylation and vacuolar acidification. *J. Cell Sci.* **123**, 3357–3367 (2010).
32. McCulloch, M.W. *et al.* Psammaplin A as a general activator of cell-based signaling assays via HDAC inhibition and studies on some bromotyrosine derivatives. *Bioorg. Med. Chem.* **17**, 2189–2198 (2009).
33. Tan, M.H. *et al.* RNA sequencing reveals a diverse and dynamic repertoire of the *Xenopus tropicalis* transcriptome over development. *Genome Res.* **23**, 201–216 (2013).
34. Inlay, M.A. *et al.* Synthesis of a photocaged tamoxifen for light-dependent activation of Cre-ER recombinase-driven gene modification. *Chem. Commun. (Camb.)* **49**, 4971–4973 (2013).



## Acknowledgments

We thank R. Dasgupta for helpful discussions, Y. Wan for critical reading of the manuscript, and H.H. Ng (Genome Institute of Singapore), R. Dasgupta (Genome Institute of Singapore), and B. Lim (Genome Institute of Singapore) for reagents. STF3A cells were a gift from D. Virshup (Duke-National University of Singapore Graduate Medical School). This work was supported by core funding from the Genome Institute of Singapore (M.H.T.), an Agency for Science Technology and Research Joint Council Office grant 1431AFG103 (M.H.T.), and a startup grant from Nanyang Technological University (M.H.T.).


## Author contributions

M.H.T. conceived the project, designed the experiments, performed the experiments, analyzed the data, supervised the research, and wrote the manuscript. K.I.L., M.N.B.R., C.W.A.W., Y.W., T.Z., B.Y.C., A.G., M.Z.H.C., J.J., and J.H.J.L. performed experiments and analyzed data. X.Z. analyzed deep-sequencing data. G.R.D.Y. provided input about the experimental design, performed the experiments, and analyzed the data.

## Competing financial interests

The authors declare competing financial interests: details are available in the online version of the paper.

## Additional information

Any supplementary information, chemical compound information and source data are available in the online version of the paper. Reprints and permissions information is available online at http://www.nature.com/reprints/index.html. Correspondence and requests for materials should be addressed to M.H.T.

© 2016 Nature America, Inc. All rights reserved.

## ONLINE METHODS

**Cell culture and transfection.** All cell lines were cultured in DMEM supplemented with 10% FBS, 2 mM L-glutamine and 1% penicillin–streptomycin. HEK293 cells were obtained from H.H. Ng, and STF3A cells were obtained from D. Virshup. The cells were routinely checked for mycoplasma contamination using a commercial detection kit (ATCC 30-1012K). Transfections were performed in 12-well plates at around 70% cell confluence using either Turbofect (Thermo Scientific) or Lipofectamine 2000 (Life Technologies), according to the manufacturers' instructions. When necessary, cells were treated with varying concentrations of 4HT (Sigma-Aldrich).

**PCR and mutagenesis.** All oligonucleotides for PCR and mutagenesis reactions were purchased from Integrated DNA Technologies (IDT). PCR was performed with MyTaq DNA Polymerase (BioLine), Phusion High-Fidelity DNA Polymerase (New England BioLabs), or Q5 High-Fidelity DNA Polymerase (New England BioLabs). For MyTaq, the following cycling parameters were used: 95 °C for 3 min; 35 cycles of 95 °C for 30 s, 60 °C for 30 s, and 72 °C for 30 s; and 72 °C for 2 min. For Phusion and Q5, the following cycling parameters were used: 98 °C for 3 min; 40 cycles of 98 °C for 15 s, 63 °C for 30 s, and 72 °C for 30 s; and 72 °C for 2 min. Mutagenesis was performed using QuikChange Lightning Site-Directed Mutagenesis kit (Agilent Technologies) according to the manufacturer's instructions in order to incorporate novel restriction sites or DNA linker fragments into our CRISPR–Cas9 variant plasmids. Mutagenic primers were designed using the QuikChange Primer Design Tool (http://www.genomics.agilent.com/primerDesignProgram.jsp).

**Construction of Cas9 variants.** The GeneArt CRISPR nuclease vector (Life Technologies), which contains a human codon-optimized *S. pyogenes* Cas9 enzyme with a V5 epitope tag, was used as the wild-type Cas9 expression plasmid. The ERT2 domain was PCR amplified from pCAG-ERT2-Cre-ERT2, which was a gift from C. Cepko (Addgene plasmid 13777), and subcloned into the pCR-BluntII-TOPO vector (Life Technologies). Different linkers and restriction sites were added using the QuikChange Lightning kit (Agilent Technologies). Each of the modified ERT2 fragment was flanked with AgeI and SfoI or EcoRI and XbaI sites for cloning into the N or C terminus of Cas9, respectively. All Cas9 variants were confirmed by Sanger sequencing.

For experiments benchmarking iCas against other conditional genome-editing systems based on post-translational control, the GeneArt vector backbone was digested with NotI and XbaI and gel purified. The intein–Cas9 enzyme was PCR amplified from pKMD111e-intein–Cas9(S219-G521R), which was a gift from D. Liu (Addgene plasmid 64192), and the split-Cas9 fragments were PCR amplified from PX851, PX852, PX853, and PX854, which were a gift from F. Zhang (Addgene plasmids 62883, 62884, 62885, and 62886 respectively). An internal XbaI site was removed from plasmid 64192 by site-directed mutagenesis using the QuikChange Lightning kit (Agilent) without changing the amino acid sequence. The intein–Cas9 construct and the split-Cas9 fragments were cloned into the GeneArt vector backbone and confirmed by Sanger sequencing.

**GFP disruption assay.** HEK293-GFP stable cells were purchased from GenTarget. One day after seeding, cells were transfected using Lipofectamine 2000 (Life Technologies) according to the manufacturer's instructions, with efficiency of at least about 70% per well. Experimental cells were treated with 1 μM 4-HT (Sigma-Aldrich), and control cells remained in culture medium devoid of 4-HT. 5 d after transfection, cells were trypsinized and resuspended in PBS containing 2% FBS for analysis by flow cytometry. Clumped or dead cells were gated out on the basis of their forward and side scatter profiles. The gate for OFP-positive cells was set on the basis of untransfected cells. All data were normalized to the average fluorescence intensity of cells transfected with a plasmid that did not express sgRNA.

**Generation of STF3A-Tet-On stable cells.** STF3A cells[30–32] were modified to stably express the Tet-On 3G transactivator protein via retroviral transduction and drug selection. Briefly, to generate retroviruses, the GP2-293 packaging cells (Clontech) were transfected at around 70% confluence with a transfection mix comprising 20 μg pCMV-VSVG vector carrying the gene encoding the viral envelope protein, 50 μg pRETROX-TET3G vector carrying the viral packaging and Tet-On 3G genes (CloneTech), and 140 μl Lipofectamine 2000 (Life Technologies) diluted in 3.75 ml Opti-MEM (Life Technologies) and 7.5 ml DMEM containing 10% FBS. The transfection mix was substituted with 10 ml DMEM containing 5% FBS after 6 h of incubation at 37 °C. Retrovirus-containing medium was harvested after 24 h and purified using Amicon Ultra-15 Centrifugal Filter Units (Merck Millipore). STF3A cells were then infected twice, with 20 μl retrovirus each time, and subsequently selected in DMEM containing 500 μg/ml G418 over 5 d. To test the expression of the transactivator gene, STF3A-Tet-On cells were transfected with 1 μg pTRE-tdTomato vector (Addgene 50798) and observed for red fluorescence 24 h after treatment with 1 μg/ml dox.

**Luciferase assay.** STF3A-Tet-On cells were transfected with 1 μg iCas or $P_{TRE3G}$-Cas9 and treated with 1 μM 4-HT or 1 μg/ml dox, respectively, for 6 h. The cells were then trypsinized and reseeded equally into a Corning 96-well flat-, clear-bottom white plate. Samples were assayed for luciferase activity using Dual-Glo Luciferase (Promega) according to the manufacturer's instructions. All measurements were taken using i-control software for Tecan microplate readers. All firefly luciferase measurements were normalized to the corresponding Renilla luciferase readings.

**Surveyor cleavage assay.** Genomic DNA was isolated from cells using the DNeasy Blood and Tissue Kit (Qiagen), and loci of interest were amplified using Q5 High-Fidelity DNA Polymerase (New England BioLabs) (see **Supplementary Table 3** for list of primers). The PCR products were purified using the GeneJET Gel Extraction Kit (Thermo Scientific). Subsequently, 250 ng DNA was incubated at 95 °C for 5 min in 1× NEBuffer 2 and then slowly cooled at a rate of −0.1 °C/s. After annealing, 5 U T7 endonuclease I (New England BioLabs) was added to each sample and the reactions were incubated at 37 °C for 50 min. The T7E1-digested products were separated on a 2.5% agarose gel stained with GelRed (Biotium), and the gel bands were quantified using ImageJ.

**Illumina deep sequencing.** Sequencing libraries were constructed via two rounds of PCR. In the first round, the loci of interest were amplified from genomic DNA using Q5 High-Fidelity DNA Polymerase (New England BioLabs) and the primers listed in **Supplementary Table 4**. Each forward primer contains the common sequence GCG TTA TCG AGG TC, and each reverse primer contains the common sequence GTG CTC TTC CGA TCT. In the second round, the PCR products from the first round were barcoded using Phusion High-Fidelity DNA Polymerase (New England BioLabs) and the following primers: forward, AAT GAT ACG GCG ACC ACC GAG ATC TAC ACC TA CAC GAG CGT TAT CGA GGT C; reverse, CAA GCA GAA GAC GGC ATA CGA GAT (barcode) GTG ACT GGA GTT CAG ACG TGT GCT CTT CCG ATC T.

10-bp barcodes designed by Fluidigm for the Access Array System were used. All samples were sequenced on MiSeq (Illumina) to produce paired 151-bp reads.

**Cell fractionation.** HEK293 cells were fractionated using the Rapid Efficient And Practical (REAP) method[35]. Briefly, the cells were scraped in ice-cold PBS, collected into 1.5-ml microcentrifuge tubes, and centrifuged for 10 s in a table-top centrifuge. The supernatant was discarded and the pellet was lysed with 0.1% Igepal CA630 (Sigma-Aldrich) in PBS supplemented with protease inhibitor (Calbiochem). Whole-cell lysates were aliquoted, and the remainder was centrifuged for 10 s. The supernatant, comprising the cytosolic fraction, was collected into a new tube. The pellet, comprising the nuclear fraction, was resuspended using 0.1% Igepal CA630 in PBS with protease inhibitor. Whole-cell lysates and nuclear fractions were subjected to 10 cycles of sonication (each cycle consisted of 30 s sonication followed by 30 s rest).

**Western blot analysis.** Proteins from whole-cell lysates, nuclear fractions, and cytosolic fractions were loaded in equal amounts for SDS–PAGE and transferred onto a nitrocellulose membrane for western blot analysis. The primary

© 2016 Nature America, Inc. All rights reserved.

antibodies used were α-V5 (Life Technologies, catalog number R960-25, 1:8,000 dilution), α-3PGDH (Santa Cruz, catalog number sc-100317, 1:1,000 dilution), and α-total histone H3 (Abcam, catalog number ab1791, 1:10,000 dilution). Primary antibodies were diluted in Tris-buffered saline containing 0.1% Tween 20 (TBST) + 5% milk and incubated overnight at 4 °C. Secondary antibodies (GE Healthcare, catalog number NA931V; Abcam, catalog number ab6721) were used at a 1:2,500 dilution in TBST + 5% milk. Membranes were exposed after addition of WesternBright Sirius HRP substrate (Advansta).

**Immunohistochemistry.** Paraformaldehyde-fixed HEK293 cells were first incubated with blocking solution (10% FBS in 0.1M PBS) (JR Scientific) for 30 min and then quenched with 3% hydrogen peroxide. Next, the samples were incubated for 2 h at room temperature or 4 °C overnight with primary antibody specific for the V5 epitope tag (Life Technologies) in blocking solution. Negative controls were incubated with blocking solution without primary antibody. Subsequently, the samples were thoroughly washed with PBS and incubated for 1 h at room temperature with secondary horseradish peroxidase (HRP)-conjugated antibody (GE Healthcare UK). After further incubation with DAB substrate (Vector Laboratories) for 10 min at room temperature, the cover slips were washed with distilled water, counter-stained with hematoxylin (Vector Laboratories) for 10 min to reveal cellular material, and mounted onto glass slides (Thermo Scientific). All slides were viewed and imaged using a light microscope (Zeiss Axio Imager Z1 with attached Leica Axiocam MRc5 camera) with the appropriate filters.

**Immunofluorescence.** HEK293-iCas cells were fixed with 4% PFA for 20 min and then washed with PBS. 1% Triton X-100 in PBS was added to permeabilize the cells, which were then incubated at room temperature for 20 min. Next, the cells were blocked with 10% FBS in TBST at room temperature for 1 h and then stained with anti-V5 antibody (Life Technologies; 1:500 dilution) at 4 °C overnight. Cells were then washed with TBST and stained with a secondary conjugated antibody (Alexa Fluor 594; 1:1,000 dilution) at room temperature for 2 h. Last, the cells were stained with Hoechst (1:10,000 dilution) at room temperature for 5 min. Images were taken using EVOS FL Imaging System (Life Technologies) at 20× magnification.

**Statistical analysis.** Statistical tests, including Student's *t*-test, Wilcoxon rank-sum test, and Kolmogorov–Smirnov test, were done as described in the figure legends. All *P* values were calculated with the R software package or Microsoft Excel. The following biological replicates were performed for **Figure 3c**: 1 replicate, *VEGFA* P1 2 and 6 h, *VEGFA* P2 2 h, *WAS* I1 2 and 24 h, *WAS* I2 2 h, *FANCF* 2 and 8 h; 2 replicates, *VEGFA* P1 0, 4, 8, and 24 h, *VEGFA* P2 0, 4, and 24 h, *WAS* I1 16 h, *WAS* I2 6 and 16 h, *TAT* 0, 6, and 16 h, *FANCF* 6 h; 3 replicates, *VEGFA* P1 16 h, *VEGFA* P2 6, 8, and 16 h, *WAS* I1 0, 4, 6, and 8 h, *WAS* I2 0, 4, and 8 h, *TAT* 2 and 8 h, *FANCF* 0, 16, and 24 h; 4 replicates, *TAT* 4 h, *FANCF* 4 h; 5 replicates, *WAS* I2 24 h, *TAT* 24 h.

35.Suzuki, K., Bose, P., Leong-Quong, R.Y., Fujita, D.J. & Riabowol, K. REAP: A two minute cell fractionation method. *BMC Res. Notes* **3**, 294 (2010).

© 2016 Nature America, Inc. All rights reserved.



doi:10.1038/nchembio.2179